diversity

MDPI

Article

A Faunistic Revision of Longnose Skates of the Genus *Dipturus* (Rajiformes: Rajidae) from the Southern Southwestern Atlantic Ocean, Based on Morphological and Molecular Evidence

Daniel Enrique Figueroa [1], Mauro Belleggia [1,2,3,*], Gabriela Andreoli [2], Silvina Izzo [2], Nelson Bovcon [4,5], Marcos Pérez-Losada [6], Agustín María De Wysiecki [3,7], Jorge Horacio Colonello [2] and María Inés Trucco [2]

1 Departamento de Ciencias Marinas, Facultad de Ciencias Exactas y Naturales, Universidad Nacional de Mar del Plata, Buenos Aires B7602AYL, Argentina; dfiguer@mdp.edu.ar
2 Instituto Nacional de Investigación y Desarrollo Pesquero (INIDEP), Paseo V. Ocampo N°1, Mar del Plata B7602HSA, Argentina; gandreoli@inidep.edu.ar (G.A.); mtrucco@inidep.edu.ar (M.I.T.)
3 Consejo Nacional de Investigaciones Científicas y Técnicas (CONICET), Avenida Rivadavia 1917, Buenos Aires C1033AAJ, Argentina; adewysiecki@cenpat-conicet.gob.ar
4 Instituto de Hidrobiología, Facultad de Ciencias Naturales y Ciencias de la Salud, Universidad Nacional de la Patagonia San Juan Bosco, Trelew 9100, Argentina
5 Instituto Multidisciplinario para la Investigación y Desarrollo Productivo y Social de la cuenca del Golfo San Jorge, Comodoro Rivadavia 9005, Argentina
6 Computational Biology Institute, Department of Biostatistics & Bioinformatics, Milken Institute School of Public Health, The George Washington University, Washington, DC 20052, USA
7 Centro para el Estudio de Sistemas Marinos (CESIMAR), Puerto Madryn U9120ACD, Argentina
* Correspondence: belleggia@inidep.edu.ar

check for updates

Citation: Figueroa, D.E.; Belleggia, M.; Andreoli, G.; Izzo, S.; Bovcon, N.; Pérez-Losada, M.; De Wysiecki, A.M.; Colonello, J.H.; Trucco, M.I. A Faunistic Revision of Longnose Skates of the Genus *Dipturus* (Rajiformes: Rajidae) from the Southern Southwestern Atlantic Ocean, Based on Morphological and Molecular Evidence. *Diversity* **2024**, *16*, 146. https://doi.org/10.3390/d16030146

Academic Editors: Bert W. Hoeksema and Simon Weigmann

Received: 10 January 2024
Revised: 21 February 2024
Accepted: 22 February 2024
Published: 25 February 2024

Abstract: The identity of longnose skates (*Dipturus-Zearaja*-like skates) in the southern cone of the Americas has been a topic of extensive debate. This study employs a comprehensive analysis encompassing morphometrics, claspers, and the examination of COI and NADH2 sequence data to conclusively demonstrate the existence of only two longnose skate species in the southwestern Atlantic Ocean, extending south of 35 °S. Notably, *Dipturus argentinensis* Díaz de Astarloa, Mabragaña, Hanner and Figueroa, 2008 is revealed as a junior synonym of *D. trachyderma* (Krefft and Stehmann, 1975). *Dipturus leptocaudus* (Krefft and Stehmann, 1975) remains a northern valid species, but the specimen from the Falkland Islands (Malvinas) is recognized as a misidentification of *D. trachyderma*. *Zearaja flavirostris* (Philippi, 1892) and *Dipturus lamillai* Concha, Caira, Ebert and Pompert, 2019 are confirmed as junior synonyms of *Zearaja brevicaudata* (Marini, 1933). These findings contradict the previous report of six species within the same region over the last decade and underscore the presence of *D. trachyderma* and *Z. brevicaudata* south of 35 °S in the southwestern Atlantic. Additionally, this study notes the occurrence of only one specimen of *Z. chilensis* (Guichenot, 1848) in the Falkland Islands (Malvinas), suggesting an unusual frequency of this eastern Pacific skate in the southern Southwest Atlantic. Given that clasper morphology serves as the key distinguishing trait between *Dipturus* and *Zearaja* species, we provided a detailed analysis of the clasper characteristics of the Atlantic *D. trachyderma*, unequivocally situating it within *Dipturus*. The diagnostic characteristics include: (i) the presence of cartilage with the distal portion referred to as the sentinel, a feature absent in *Zearaja*; (ii) longer ventral terminal cartilage with the distal end referred to as the funnel, compared to *Zearaja*; and (iii) a non-spatulate distal lobe, a distinctive trait specific to *Dipturus*.

Keywords: biodiversity; systematics; *Zearaja*; Argentina; genetic; anatomy

1. Introduction

Longnose skates (*Dipturus-Zearaja*-like skates) are mostly found on continental shelves and slopes within cool temperate to tropical waters [1]. Of the 38 longnose skate species described worldwide to date [2,3], 7 have been reported in the southwestern Atlantic and

southeastern Pacific regions (specifically Argentina and Chile) south of 35 °S. These species include *Dipturus lamillai* Concha, Caira, Ebert and Pompert, 2019, *Dipturus leptocaudus* (Krefft and Stehmann, 1975), *Dipturus trachyderma* (Krefft and Stehmann, 1975), *Zearaja argentinensis* (Díaz de Astarloa, Mabragaña, Hanner and Figueroa, 2008), *Zearaja brevicaudata* (Marini, 1933), *Zearaja chilensis* (Guichenot, 1848) and *Zearaja flavirostris* (Philippi, 1892). A notable and evident distinction between the *Dipturus* and *Zearaja* genera lies in the morphology of the clasper, specifically the absence of the accessory terminal 1 cartilage (at1) in *Zearaja* [4,5].

The presence of the *Zearaja* species in the southern cone of the Americas has been a matter of discussion over the last decade. Initially, in a comprehensive survey of elasmobranch DNA sequences worldwide, Naylor et al. [6] identified differences in longnose skate *Zearaja* specimens from the Pacific (commonly referred to as *Z. chilensis*) and three specimens from the Atlantic (commonly referred to as *Z. flavirostris*). Subsequently, Gabbanelli et al. [7] demonstrated distinctions between specimens from the Southwest Atlantic and the Southeast Pacific by comparing external morphology, spinulation patterns, claspers, egg cases, and mitochondrial cytochrome c oxidase I (COI) sequence data. Through these analyses, *Z. brevicaudata* was resurrected from synonymy with *Z. chilensis* and *Z. flavirostris* in the Southwest Atlantic [7]. Concurrently, Concha et al. [5], using NADH dehydrogenase subunit 2 (NADH2) sequence data, identified Southwest Atlantic specimens as a novel cryptic species, subsequently described as *D. lamillai*. It was clarified that *D. lamillai* was a junior synonym of *Z. brevicaudata*, resolving the confusion between these two species [3].

Conversely, the giant bi-oceanic longnose roughskin skate *D. trachyderma* was initially described from a pre-adult male captured in the southwestern Atlantic [8]. Subsequently, Leible and Stehmann [9] reported the presence of this giant skate in the southeastern Pacific, providing a detailed description of juvenile and adult specimens from both sexes, along with a comprehensive clasper description. Molecular studies were also conducted in this oceanic sector [10]. *Dipturus argentinensis*, originally described based on morphology and DNA barcoding from ten juvenile specimens ranging from 403 to 935 mm total length collected off Patagonia, Argentina [11], was renamed *Z. argentinensis* based on molecular studies [2,12]. Similarly, the longnose skate *D. leptocaudus* was described from juveniles from southern Brazil [8], and Naylor et al. [6], in their extensive survey of elasmobranch DNA sequences collected worldwide, included samples of this species from the Falkland Islands (Malvinas). Recent analyses by Carugati et al. [13] focused on COI sequences of the *Dipturus* genus from public repositories, revealing that a sequence of *D. trachyderma* was recognized as *D. argentinensis*. Additionally, Concha [14] encountered an unexpected grouping of *D. trachyderma* with 12 juveniles of *Z. argentinensis*.

In light of the intricate findings above, the goal of this study was to analyze and compare the morphology, along with DNA sequences of the two mtDNA genes COI and NADH2, of the most frequently encountered *Zearaja* and *Dipturus* species in the southern cone of the Americas, aiming to provide clarity on their taxonomic status.

2. Materials and Methods

2.1. Sampling and Morphometrics

Specimens were collected from various locations in the Southwest Atlantic spanning the years 2005 to 2022. Collections efforts were carried out through both commercial fishing vessels and scientific trawl surveys conducted by the research vessels "Dr. Eduardo Holmberg" and "Victor Angelescu" of the Instituto Nacional de Investigación y Desarrollo Pesquero (INIDEP, Argentina). Four specimens of *D. trachyderma* underwent sex determination, were weighted to the nearest gram (total weight, TW), and measured to the nearest millimeter (the total length, TL, and disc width, DW). The maturity stage of the specimens (adult, preadult, and juvenile) was recorded following the criteria in Walker [15] and Colonello et al. [16]. Males were classified as juvenile, preadult, or adult based on clasper calcification, testes development, and convoluted sperm ducts. Females were classified based on the presence of eggs in the uteri and the condition of the oviduc-

tal gland, uteri, and oocytes [17]. One specimen (VictI) was preserved in the collection of the Instituto de Hidrobiología, Universidad Nacional de la Patagonia San Juan Bosco (UNPSJB-ICT) and assigned number 2005/57 (Table 1). External measurements and counts followed the methodology outlined in Krefft and Stehmann [8]. The terminology used for dermal structures morphology follows Weigmann and Reinecke [18]. Differentiation between thorns and thornlets is based on their size: thornlets are similar in shape but larger and more robust than denticles, and thorns double thornlets in size and height [18]. For clasper analysis, radiographs were obtained using a Philips Digital Diagnost Series RX197 digital X-ray system at the Instituto Radiológico Mar del Plata, Argentina. Additionally, measurements and analyses were performed on the holotype of *D. argentinensis* (INIDEP No. 793), paratypes of *D. argentinensis* (INIDEP No. 796, 798, 799), and preadults of *D. trachyderma* (INIDEP No. 789). External measurements of the *D. trachyderma* holotype (ZMH 25,402–ex ISH 130/71) were reconstructed based on the percentages provided in the original description [8].

To facilitate morphological comparisons between *D. trachyderma* and *D. argentinensis*, external measurements were normalized to remove allometric effects of body size, following Lleonart et al. [19]. Total length was used as the independent variable, while disc width and length; snout length; orbit diameter and length; spiracle length; distance between spiracles; mouth width; distance between nostrils; width of the first, third, and fifth gill openings; distance between both the first and fifth gill openings; height of the first dorsal fin; length of both the first and second dorsal fin base; interdorsal distance; and distance from the cloaca to the first and second dorsal fins, caudal tip, and snout were considered as dependent variables. The normalized values were used to construct a Bray–Curtis dissimilarity matrix [20,21], where a high value in the dissimilarity matrix indicates dissimilarity between two specimens [21]. To visualize the dissimilarity matrix in two-dimensional configurations, a non-metric multidimensional scaling ordination (nMDS) was used to group the specimens [21]. Points close to each other on the nMDS ordination diagram represent specimens that are more similar, while those farther apart are less similar [21]. All statistical analyses were performed using the open-source R language, with libraries "MASS" and "vegan".

2.2. Genetic Data Analysis

A total of 32 skate specimens were collected during INIDEP's research cruises and commercial landings between 2012 and 2018 for molecular analyses (Table 1). The skates were initially identified on board as *D. argentinensis*, *D. trachyderma*, and *Z. brevicaudata* (previously also known as *Z. flavirostris* during the sampling period), following Figueroa [22]. COI gene sequences were obtained from 13 specimens (5 *D. argentinensis*, 2 *D. trachyderma*, and 6 *Z. brevicaudata*), while NADH2 sequences were obtained from 26 specimens (5 *D. argentinensis*, 4 *D. trachyderma*, and 17 *Z. brevicaudata*) (Table 1).

A muscle tissue sample of each specimen was preserved in 96% ethanol, and DNA extraction was carried out using phenol-chloroform-isoamyl alcohol, following the protocol proposed by Andreoli and Trucco [23]. Amplification of a fragment ranging from 700 to 800 bp of the COI gene and 800 to 900 bp of the NADH2 gene was achieved through PCR using gene-specific primers. For COI, the forward and reverse primers were FishF2 (5′TCGACTAATCATAAAGATATCGGCAC3′) and FishR1 (5′TAGACTTCTGGGTGGCCAAAGAATCA3′), respectively [24], while for NADH2, they were ILEM (5′AAGGAGCAGTTTGATAGAGT3′) and reverse ASNM (5′ACGCTTAGCTGTTAATTAA3′), respectively [25]. Each PCR reaction was performed in a final volume of 25 µL, comprising 1X PCR buffer, 1.5 mM MgCl2, 0.2 mM dNTPs; 0.2 µM of each primer, 0.125 U Taq polymerase T-free, 5 µL of DNA (dilution 1:10), and ultrapure water up to the final volume. The amplification was performed in a BioerLife Express TC-96/G/H thermocycler under the following conditions: initial denaturation at 95° for 2 min; 35 cycles of denaturation at 94 °C for 1 min, annealing at 56 °C (NADH2) or 54 °C (COI) for 1 min, and extension at 72 °C for 2 min, and a final extension at 72 °C for 15 min with a pause at 6 °C. PCR products were visualized through

1.5% agarose gels electrophoresis stained with 0.01% ethidium bromide. The purified products were sequenced bidirectionally at Macrogen (South Korea) using the same primers used for gene amplification. The sequences obtained in this work and accession numbers are listed in Table 1. Sequences of *D. trachyderma*, *D. argentinensis*, *Z. flavirostris*, *Z. nasuta* (Müller and Henle, 1841), *D. leptocaudus*, and *Z. chilensis* with different distributions in the southern hemisphere were taken from the BOLD and Genbank databases as reference sequences (Tables S1 and S2). Due to the absence of *D. lamillai* COI gene sequences in public databases, the COI gene was extracted from the complete mitochondrial genome of *Z. chilensis* published under the accession number (Genbank KF648508-Z. chilensis) [26], which nested within *D. lamillai* cluster species in a previous NADH2 analysis [5].

Chromatograms were manually checked for errors and ambiguous base calls using Bioedit Sequence Alignment Editor Software version 7.1.3.0 [27]. The COI and NADH2 sequences underwent cross-referencing with sequences taken from the database through a BLASTn analysis on Genbank (Basic Local Alignment Search Tool) to confirm their taxonomic identity. For each gene, a multiple alignment was created with the ClustalW 2.0 program [28] using default settings. To determinate genetic divergences among species, interspecific K2P distances were calculated [29]. Different groups were defined for resolving controversial taxonomic statuses as follows: *D. trachyderma*, *D. argentinensis*, *Z. flavirostris*, *D. lamillai*, *Z. brevicaudata*, *Z. chilensis*, and *Z. nasuta* for COI; and *D. trachyderma*, *D. argentinensis*, *Z. flavirostris*, *D. lamillai*, *Z. chilensis*, *Z. nasuta*, *D. leptocaudus* (JQ518866.1, [6]), and *D. lamillai* (KF648508.1, [26]) for NADH2. Distances < 0.5% were considered indicative of the same species [24].

The best substitution model was found for COI and NADH2 sequences, being the K2P model for COI and the Hasegawa–Kishino–Yano (HKY) model for NADH2, both with a gamma distribution of rates among sites. Maximum likelihood (ML) trees were carried out using these models with 1000 bootstrap replicates to evaluate tree topology in the MEGA 6 program [30]. To explore intraspecific diversity and its relationship with geographic distribution, median-joining networks of haplotypes were constructed for COI (Table S3) and NADH2 (Table S4). The haplotype analysis was performed using Dnasp 5.1 [31] and Network 10.2 software [32].

Table 1. Samples of *Dipturus* and *Zearaja* specimens sequenced for genetic analysis in this study. The table includes sample id, species identification by morphology, collector information, and COI and NADH2 Genbank accession numbers. (*) Izzo et al. [33].

	Sample ID	Species Identification by Morphology	Collector	Accession No.	
				COI	NADH2
1	EH0113 L13	*D. argentinensis*	INIDEP EH01/13	OR712800	OR813832
2	EH0113 L9	*D. argentinensis*	INIDEP EH01/13	OR712799	OR813828
3	EH0117 L13-3	*D. argentinensis*	INIDEP EH01/17	OR712798	OR813834
4	EH0117 L3-1	*D. argentinensis*	INIDEP EH01/17	OR712796	OR813833
5	EH0117 L6-2	*D. argentinensis*	INIDEP EH01/17	OR712797	OR813830
6	DT7-16	*D. trachyderma*	INIDEP SW Atlantic	-	OR813835
7	EH0117 L6	*D. trachyderma*	INIDEP EH01/17	OR712801	OR813831
8	EH0118	*D. trachyderma*	INIDEP EH01/18	-	OR813829
9	EH0111-222	*Z. flavirostris*	INIDEP EH01/11	*	OR909869
10	EH0111-227	*Z. flavirostris*	INIDEP EH01/11	*	OR909870
11	EH0312-1	*Z. flavirostris*	INIDEP EH03/12	*	OR909871
12	EH0312-2	*Z. flsvirostris*	INIDEP EH03/12	*	OR909855
13	EH0312-3	*Z. flavirostris*	INIDEP EH03/12	*	OR909856
14	EH0312-4	*Z. flavirostris*	INIDEP EH03/12	*	OR909857
15	EH0312-5	*Z. flavirostris*	INIDEP EH03/12	*	OR909858
16	EH0312-6	*Z. flavirostris*	INIDEP EH03/12	*	OR909859
17	EH0413-1	*Z. flavirostris*	INIDEP EH04/13	*	OR909860
18	EH0413-10	*Z. flavirostris*	INIDEP EH04/13	*	OR909867

Table 1. *Cont.*

	Sample ID	Species Identification by Morphology	Collector	Accession No.	
				COI	NADH2
19	EH0413-2	*Z. flavirostris*	INIDEP EH04/13	*	OR909861
20	EH0413-4	*Z. flavirostris*	INIDEP EH04/13	*	OR909868
21	EH0413-5	*Z. flavirostris*	INIDEP EH04/13	*	OR909862
22	EH0413-6	*Z. flavirostris*	INIDEP EH04/13	*	OR909863
23	EH0413-7	*Z. flavirostris*	INIDEP EH04/13	*	OR909864
24	EH0413-8	*Z. flavirostris*	INIDEP EH04/13	*	OR909865
25	EH0413-9	*Z. flavirostris*	INIDEP EH04/13	*	OR909866
26	VictI	*D. trachyderma*	Comm. Vessel Victoria I	OR712795	OR813836
27	Zchil	*Z. brevicaudata*	Comm. Vessel Victoria I	PP024982	-
28	Zchil-1	*Z. brevicaudata*	Comm. Vessel Maria Rita	PP024983	-
29	Zchil-2	*Z. brevicaudata*	Comm. Vessel Maria Rita	PP024984	-
30	Zchil-4	*Z. brevicaudata*	Comm. Vessel Maria Rita	PP024985	-
31	Zchil-5	*Z. brevicaudata*	Comm. Vessel Maria Rita	PP024986	-
32	EH0116 L8	*Z. flavirostris*	INIDEP EH01/16	PP318455	-

3. Results

3.1. Dipturus Trachyderma Diagnosis

Juveniles (previously known as *D. argentinensis*) display a dorsal disc surface of a brownish-purple color, without distinct ocelli or blotches but bordered with dark brown on the pectoral and pelvic fins (Figure 1a,b). The upper surface of the disc is generally smooth, with only a few scattered thornlets (small dermal structures that may resemble thorns but are often barely larger than denticles) on the snout's tip. Ocular thorns are present, while scapular thorns are absent. The presence of a single nuchal thorn may vary. Typically, there is one median row of 10 to 24 small caudal thorns. The dorsal and caudal fins have very few scattered thornlets. One or two interdorsal thorns may be observed. The tail is relatively long and thin, representing approximately half of the total length. The ventral surface of the disc is as dark as the upper side, smooth, with only a few small scattered thornlets on the snout's tip. There are no thornlets in the interbranchial space. The upper surface of the disc exhibits a plain purplish-brown color, bordered with dark brown on the pectoral and pelvic fins, and lacks distinct ocelli or blotches. Thorns are marked with a pale milky-white pigment. The lateral tail folds display a creamy white pigment. The dorsal fins are uniformly brown. The lower surface of the disc is brownish in the central part, transitioning to a paler brown on the outer parts of the pectoral fins, with darker margins. The anterior lobes of the pelvic fins are dark brown, while the posterior ones are lighter and narrowly edged in grey. The underside of the tail is uniformly brown with light margins at the level of the dorsal fins (Figure 1a,b).

The preserved preadult specimens of *D. trachyderma* exhibited a thorn and color pattern akin to that observed in the holotype, with the exception of having more than one dorsal row of tail thorns (Figure 1c,d). Occasionally, one row is present on each side of the tail's midline, and at times, a second row sparsely forms on each side of the tail's midline. The dorsal surface of the disc is rough due to a dense lining of thornlets, almost thorns, concentrated in the central region of the trunk. These are widely scattered only on the posterior half of the pectoral fins, giving the impression of a thornlet-free posterior region (Figure 1c,d). The outer lobes of the pelvic fins, the dorsal part of the tail, and both the dorsal and caudal fins have large scattered thornlets. Thorn presence includes two preorbital, two interorbital, one postorbital, and one interspiracular. The dorsal part of the tail features a central row of 26–29 thorns of different sizes, and one or two lateral rows begin to form on each side of the central thorn's midline. The ventral side of the disc is notably rough, spiny, and densely covered on the rostrum, along the rostral halves of the anterior edge of the disc, and around the mouth and the nasal openings. The remaining parts of the head, including the interbranchial space, show scattered spination. The nasal

flap's half is smooth, surrounded by a wide strip of widely spaced thornlets. The anal region and the middle parts of the posterior lobes of the pelvic fins are scattered spined and rough. The underside of the tail is covered with irregularly spaced thornlets up to the tail's tip. The dorsal side is uniformly dark gray-brown, slightly lighter on both sides of the rostral cartilage and in the interorbital space. On the dorsal part of the trunk, a wide stripe of the same color extends from the tips of the pectoral fins along the posterior edge of the disc to the axes of these fins. The pelvic fins are darker than the disc, with a narrow pale border on the anterior edge of the anterior apical lobe. The caudal and dorsal fins match the disc's dark color, without transparent areas. The basic color of the abdominal part is mainly dark gray-brown, more intense on the anterior part. The tip of the snout, edges of the nasal openings, and nasal clefts are black, the lower jaw is very dark brown, with bright white teeth, and the gill openings are a dull grayish-white. A wide stripe from the apices of the pectoral fins to the axes of these fins is of medium gray color, clearly contrasting with the rest of the disc's color. All mucous pores are marked in black but are difficult to distinguish in the disc's dark color. In the snout region, as well as on the upper and lower jaws, the pores appear very dense, while they are irregularly and sparsely distributed on the disc.

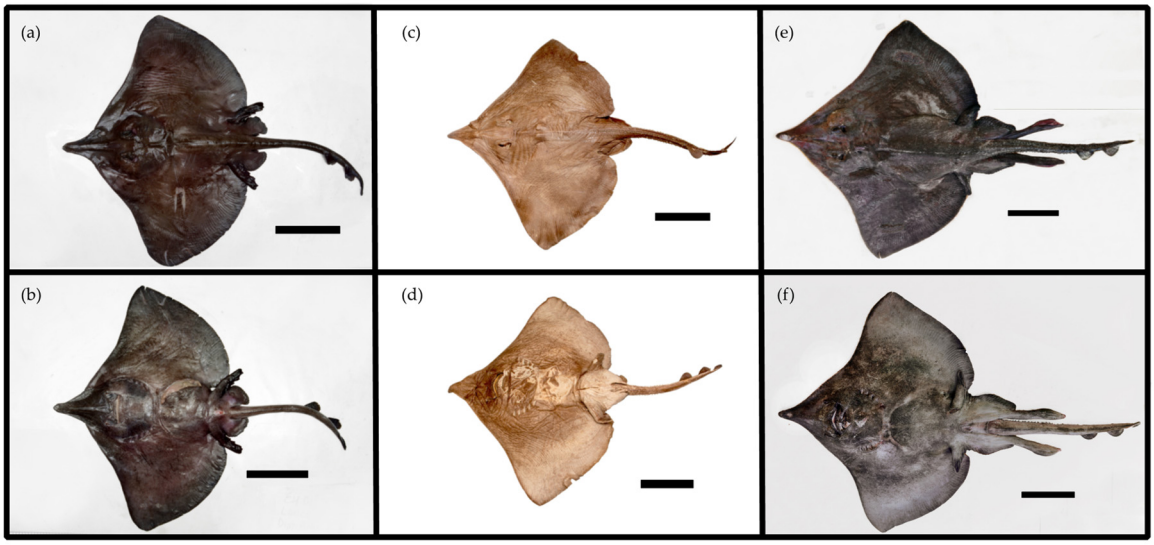

Figure 1. (**a**) dorsal view of *D. argentinensis* (EH0117 L6-2) juvenile male, total length (TL) 505 mm, disc width (DW) 376 mm, and total weight (TW) 684 g; (**b**) ventral view of *D. argentinensis* (EH0117 L6-2) juvenile male, TL 505 mm, DW 376 mm, and TW 684 g; (**c**) dorsal view of *D. trachyderma* (INIDEP 789) preadult male, TL 1211 mm, and DW 933 mm; (**d**) ventral view of *D. trachyderma* (INIDEP 789) preadult male, TL 1211 mm, and DW 933 mm; (**e**) dorsal view of *D. trachyderma* (DT7-16) adult male, TL 2135 mm, DW 1480 mm, and TW 48,100 g; and (**f**) ventral view of *D. trachyderma* (DT7-16) adult male, TL 2135 mm, DW 1480 mm, TW 48,100 g. Scale bar in (**a**,**b**) is 100 mm and in (**c**–**f**) is 300 mm.

Adults of both sexes are distinguished by the presence of coarse thornlets covering their upper and lower surfaces, with no distinct thorns on the upper disc (Figure 1e,f). In adult males, there is a reduction in thornlets on the dorsal pectoral centers, resulting in a largely smooth area surrounded by broad bands of thornlets along the disc margins and the posterior part of the trunk (Figure 1e,f). Scattered irregularly across the disc, a few larger thornlets, resembling thorns, can be found, particularly in larger specimens (Figure 1e,f). The pelvic fins, sides of the tail, dorsal and caudal fins, as well as mature male claspers, are also covered by thornlets. The ventral surface is also predominantly rough, with the exception of the smooth belly. Thornlets are densely packed on the snout, particularly along the rostrum and outer margins, as well as on the sides of the mouth. Thornlets are somewhat sparsely scattered on the pelvic fins, claspers, and the underside of the tail. As a consequence of this, the scientific name is derived, referring to the exceptionally rough

spinulation of this species. Thorns on the upper side are generally not well defined, with none of the few present at the orbital rims exceeding the size of thorns. There are no further thorns or thorns on the upper disc, particularly with the absence of nuchal thorns, except for the alar thorns in adult males. Depending on the maturity stage, males display a total of 17 up to a maximum of 48 alar thorns at each wingtip. Adults have five rows of tail thorns, consisting of one median row and two parallel lateral rows on each side, which may sometimes be irregularly arranged. The dorsal surface is uniformly dark brown without any pattern, with only mucus pores marked in black. The ventral surface is blackish in large areas, partly due to coverage with a secondary black mucus layer. The base color ranges from reddish to dark brown, especially at the posterior disc margins, on the abdomen, posterior pelvic lobes, and on the underside of the tail. Only the jaws, gill slits, and cloaca are marked in creamy white. Additionally, ventral pores are marked in black, although they are indistinct due to the dark base color (Figure 1e,f).

3.2. Clasper Morphology

The external components of the clasper of the giant Atlantic roughskin skate *D. trachyderma* did not differ in shape and had the same external and internal components as *D. trachyderma* from the Pacific. The inner surface of the exposed glans reveals distinctive features. On the inner dorsal lobe, there is a pseudorhipidion (pr) along the midline proximally, accompanied by a deep proximal cleft (cl) and a diagonal slit (sl) overlying the latter. Additionally, there is another longitudinal distal cl at midline, extending laterally as a broadly oval shallow groove on the inner surface of the dorsal lobe. A terminal bridge (tb) separates the proximal and the distal cl (Figure 2). Moving to the inner ventral lobe, several features are observed: a long shield (sh) laterally along the proximal two-thirds of the glans with a cutting outer edge of free cartilage. Its surface is covered by a diagonally pleated thin integument. Along the inner edge of the sh in its proximal two-thirds runs a monolobed, narrow rhipidion (rh) with a porous surface, somewhat widening distad. Notably, a sentinel (st) and spike (sk) are located at the midline distally between the ends of the rh and sh, with the sk extending somewhat beyond the se and below the latter. Both are rather bluntly tipped, being narrowly spoon-shaped or spatulate (Figure 2). The sentina (sn) is an oval membranous slit without cartilage support, only observable in the open clasper, as it is concealed beneath the tip of the sk, the st, and the vertical convex inner wall of the sh (Figure 2). The distal tip of the sk at the midline and extending half way to the glans tip features a puffed-up integumental roll, known as the component pad (pd), which can be recognized only in fresh or properly preserved claspers (Figure 2).

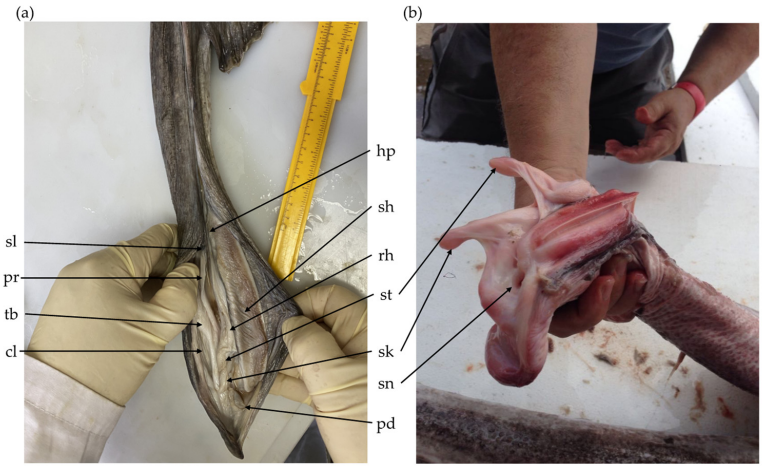

Figure 2. Opened claspers of (**a**) *Dipturus trachyderma* (DT7-16) adult male from the southwest Atlantic, total length (TL) 2135 mm, disc width (DW) 1480 mm, and total weight (TW) 48,100 g, right clasper; and (**b**) *D. trachyderma* (EH0118) adult male from the southwest Atlantic, TL 1767 mm, and DW 1341 mm, right clasper. sl: slit, pr: pseudorhipidion, tb: terminal bridge, cl: cleft, hp: hypopyle, sh: shield, rh: rhipidion, st: sentinel, sk: spike, sn: sentina, pd: pad.

The internal components that define the genus *Dipturus* were clearly observed (Figure 3). The accessory terminal 1 (at1) and sentinel (distal region of at1) cartilages were present (Figure 3). The ventral terminal (vt) and dorsal terminal 2 (dt2) cartilages were long (Figure 3). The funnel, which is the distal portion of the vt, was present (Figure 3). The distal lobe was not spatulate (Figure 3).

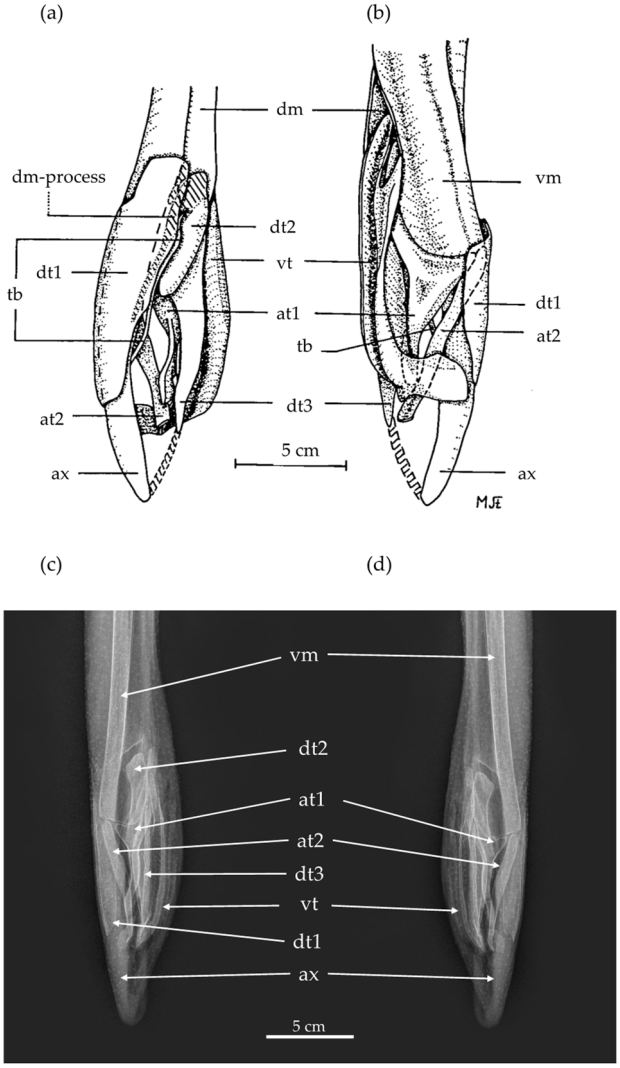

Figure 3. Original *Dipturus trachyderma* clasper description from the Pacific specimen, adult male of total length (TL) 2080 mm, right clasper, reprinted and adapted from Leible and Stehmann [9], (**a**) dorsal view and (**b**) ventral view. Radiographs of the right clasper of *D. trachyderma* (DT7-16) adult male, from the southwest Atlantic, TL 2135 mm, disc width 1480 mm, and total weight 48,100 g, (**c**) dorsal view and (**d**) ventral view. dm: dorsal marginal; vm: ventral marginal; at1: accessory terminal 1; at2: accessory terminal 2; vt: ventral terminal; ax: axial; dt1: dorsal terminal 1; dt2: dorsal terminal 2; dt3: dorsal terminal 3; tb: terminal bridge.

3.3. Morphometrics and Meristics

The two adult *D. trachyderma* specimens analyzed ranged from 1,767 to 2,135 mm TL, while the two preadults ranged from 1265 to 1513 mm TL (Table 2). These preadults of *D. trachyderma* exhibited similar morphometrics ranges to those registered in the preadult of *D. trachyderma* (INIDEP 789, 1211 mm TL) and the *D. trachyderma* holotype (ZMH 25,402–ex ISH 130/71, 1135 mm TL). The holotype and paratypes of the juvenile *D. argentinensis* measured ranged from 393 to 765 mm TL (INIDEP No. 793, 796, 798, and 799) (Table 2). The nMDS plot indicates that the measured specimens of *D. trachyderma* and *D. argentinensis* did not exhibit differences (Figure 4).

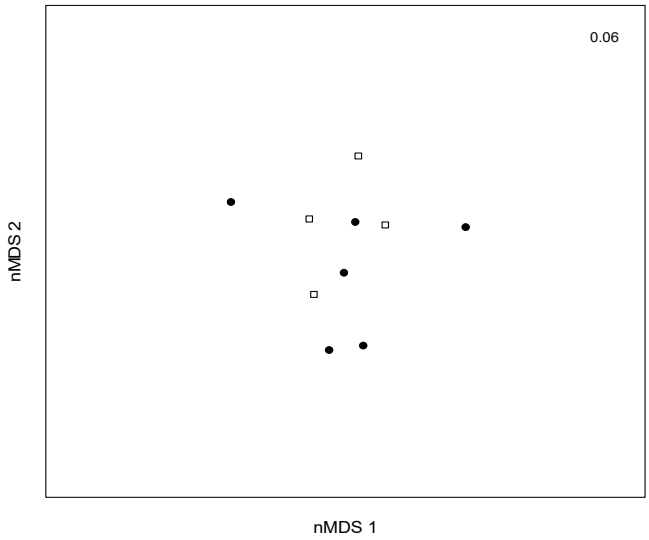

Figure 4. Non-metric multidimensional scaling (nMDS) ordination based on the Bray–Curtis dissimilarity index for the external measurements of *Dipturus trachyderma* (black circles) and *Dipturus argentinensis* (white squares). Each point on the plot represents one specimen. The 2D-stress coefficient is shown in the top right of the figure.

3.4. Molecular Analysis of COI Sequences

The results of the COI gene analysis were based on a total of 77 sequences, comprising 65 obtained from the databases, including those corresponding to additional groups and 12 sequences from the present study (Table S1).

The maximum likelihood tree of the COI sequences revealed three well-defined clusters supported by high bootstrap values (>90) (Figure 5). Firstly, group 1 comprised sequences of specimens initially classified as *Z. flavirostris* (Philippi, 1892) and *Z. brevicaudata*, forming a single clade of 36 sequences with a 99% bootstrap value (Figure 5). Group 2, with a 96% bootstrap value, consisted of 14 sequences of specimens classified as *D. argentinensis* and *D. trachyderma* (Figure 5). The clear separation from the rest of the species in the tree suggests that these specimens may correspond to the same species (Figure 5). Group 3 included two distinct clades from the Pacific (98% bootstrap value), one with sequences belonging to *Z. nasuta* and the other with sequences from *Z. chilensis* specimens (Figure 5).

The interspecific K2P distance among *D. lamillai*, *Z. brevicaudata*, and *Z. flavirostris* ranged from 0.22% to 0.33% (Table 3). The interspecific distance between *D. trachyderma* and *D. argentinensis* was 0.04% (Table 3).

The haplotype network displayed four haplogroups (Group A, B, C, and D, Figure 6). Group A (*Z. brevicaudata*) included eight haplotypes, encompassing all sequences of specimens morphologically identified as *Z. brevicaudata*, *Z. flavirostris*, and *D. lamillai* (Figure 6). The sequence KH648508.1 of *D. lamillai* shared a haplotype with sequences of specimens captured in Patagonia (HB3, Figure 6). All these sequences belonged to specimens with a distribution in the Southwest Atlantic (Figure 6). Group B consisted of two haplotypes with the sequences of specimens morphologically classified as *D. trachyderma* and *D. argentinensis* (Figure 6). This group exhibited both Pacific and Atlantic distribution (Figure 6). Group C comprised *Z. chilensis* sequences exclusively from the Pacific with a single haplotype (Figure 6). Lastly, group D, with five haplotypes, corresponded to sequences of *Z. nasuta*, which is exclusively distributed in New Zealand (Figure 6).

Table 2. Morphometrics for specimens of *Dipturus trachyderma* (D.tra) collected off the Southwest Atlantic. Values are expressed in percentage of total length, except total length that is expressed in millimeters (mm). D.arg = *Dipturus argentinensis*.

	DT7-16 D.tra	**EH0118 D.tra**	**VA01/22 D.tra**	**VictI D.tra (UNPSJB-ICT-2005/57)**	**INIDEP 789 D.tra**	**ZMH 25,402–ex ISH130/71 D.tra (Holotype)**	**INIDEP 793 D.arg (Holotype)**	**INIDEP 796 D.arg (Paratype)**	**INIDEP 798 D.arg (Paratype)**	**INIDEP 799 D.arg (Paratype)**
Sex	Male	Male	Female	Male	Male	Male	Male	Male	Male	Male
Maturity stage	Adult	Adult	Preadult	Preadult	Preadult	Preadult	Juvenile	Juvenile	Juvenile	Juvenile
Total length	2135	1767	1513	1265	1211	1135	765	705	550	393
Disc width	69.32	75.89	75.88	75.49	77.04	72.69	74.77	75.18	73.82	74.30
Disc length	55.27	62.14	77.99	57.71	59.04	59.30	60.52	63.83	56.73	57.00
Snout length (preorbital)	17.00	-	21.15	19.76	18.99	20.97	22.88	21.56	20.36	17.81
Snout length (preoral)	14.89	15.96	21.28	19.37	17.51	20.53	22.61	22.84	20.55	19.08
Orbit diameter	1.59	1.70	2.72	1.58	1.49	1.90	3.14	2.98	3.27	3.56
Distance between orbits	5.53	8.21	6.15	6.25	5.78	-	5.10	5.96	5.64	5.60
Orbit length	4.03	4.41	4.34	4.39	4.71	4.30	4.44	4.54	4.91	5.09
Spiracle length	2.86	2.26	2.58	2.35	1.98	2.40	2.88	2.41	2.00	2.54
Distance between spiracles	5.85	7.13	6.35	6.98	6.69	6.49	6.01	6.10	6.55	6.62
Mouth width	8.71	9.45	8.76	9.30	9.00	8.49	8.10	8.51	8.18	9.67
Distance between nostrils	8.24	9.05	9.39	9.16	9.08	9.50	8.76	9.22	8.73	9.92
1st gill openings width	0.98	1.41	1.55	1.57	1.57	1.69	1.96	1.84	1.64	1.78
2nd gill openings width	1.41	1.53	2.05	1.75	1.73	-	2.09	2.13	1.64	2.04
3rd gill openings width	1.59	1.64	2.12	1.90	1.98	1.89	2.09	2.13	1.64	2.04
4th gill openings width	1.59	1.75	1.92	1.76	1.73	-	1.96	1.99	1.64	2.04
5th gill openings width	1.08	1.47	1.52	1.38	0.91	1.20	1.83	1.84	1.45	1.78

Table 2. *Cont.*

	DT7-16 D.tra	EH0118 D.tra	VA01/22 D.tra	VictI D.tra (UNPSJB-ICT-2005/57)	INIDEP 789 D.tra	ZMH 25,402–ex ISH130/71 D.tra (Holotype)	INIDEP 793 D.arg (Holotype)	INIDEP 796 D.arg (Paratype)	INIDEP 798 D.arg (Paratype)	INIDEP 799 D.arg (Paratype)
1st gill openings distance	14.05	16.69	17.85	17.15	17.42	16.10	15.56	16.31	16.00	16.79
3rd gill openings distance	11.80	15.00	15.27	14.55	14.78	-	13.33	13.90	13.45	13.99
5th gill openings distance	8.81	9.73	10.97	10.43	10.82	10.40	9.28	10.07	9.64	10.94
1st dorsal fin height	3.19	3.90	3.90	3.34	3.55	3.80	3.53	3.69	3.45	3.82
1st dorsal fin base length	5.81	6.00	5.55	5.04	5.62	6.10	5.62	5.82	5.64	5.34
2nd dorsal fin height	3.23	-	3.11	3.25	3.06	3.20	3.53	3.69	3.27	3.31
2nd dorsal fin base fin length	5.39	4.24	5.35	5.41	5.20	5.30	5.36	5.39	4.91	5.60
Caudal fin height	0.75	-	0.86	0.83	0.58	-	0.78	1.13	0.91	1.27
Caudal fin base length	4.36	-	3.77	4.48	4.87	-	4.18	4.40	5.09	6.36
Interdorsal distance	1.64	1.64	1.35	2.65	1.98	1.30	1.57	1.13	1.82	1.53
Tail width at axil of pelvic fin	5.85	6.17	3.57	3.88	4.95	-	3.27	3.97	3.64	4.07
Tail width at 1st dorsal fin base	2.44	2.94	2.54	2.23	2.48	-	-	1.84	1.82	2.29
Anterior pelvic fin length	-	10.30	4.76	10.18	10.16	9.59	10.98	12.06	11.64	12.47
Snout to 1st dorsal	81.73	86.08	84.86	75.10	82.58	-	80.26	81.56	81.45	80.92
Cloaca to caudal tip	48.10	45.27	44.42	44.66	46.41	45.20	45.10	44.96	46.18	46.31
2nd dorsal fin to caudal tip	-	-	10.24	4.60	5.45	5.09	4.58	5.11	6.18	6.87
Snout to cloaca	50.82	54.78	54.53	53.75	52.44	55.80	54.90	52.91	50.18	50.64

Table 2. *Cont.*

	DT7-16 D.tra	EH0118 D.tra	VA01/22 D.tra	VictI D.tra (UNPSJB-ICT-2005/57)	INIDEP 789 D.tra	ZMH 25,402–ex ISH130/71 D.tra (Holotype)	INIDEP 793 D.arg (Holotype)	INIDEP 796 D.arg (Paratype)	INIDEP 798 D.arg (Paratype)	INIDEP 799 D.arg (Paratype)
Cloaca to 1st dorsal fin	30.44	31.30	28.62	26.17	27.33	26.90	27.58	27.66	28.18	28.75
Cloaca to 2nd dorsal fin	37.94	39.56	35.29	34.55	35.43	34.40	34.77	34.75	36.18	35.37
Inner side clasper length	26.93	25.18	-	5.75	5.78	-	4.71	4.68	3.82	3.82
Inner side clasper length from cloaca	-	-	-	8.89	9.91	9.87	-	8.51	7.64	7.12
Upper jaw tooth rows	41	34	43	41	38	38	37	35	34	38
Lower jaw tooth rows	44	36	43	40	38	38	38	33	32	34

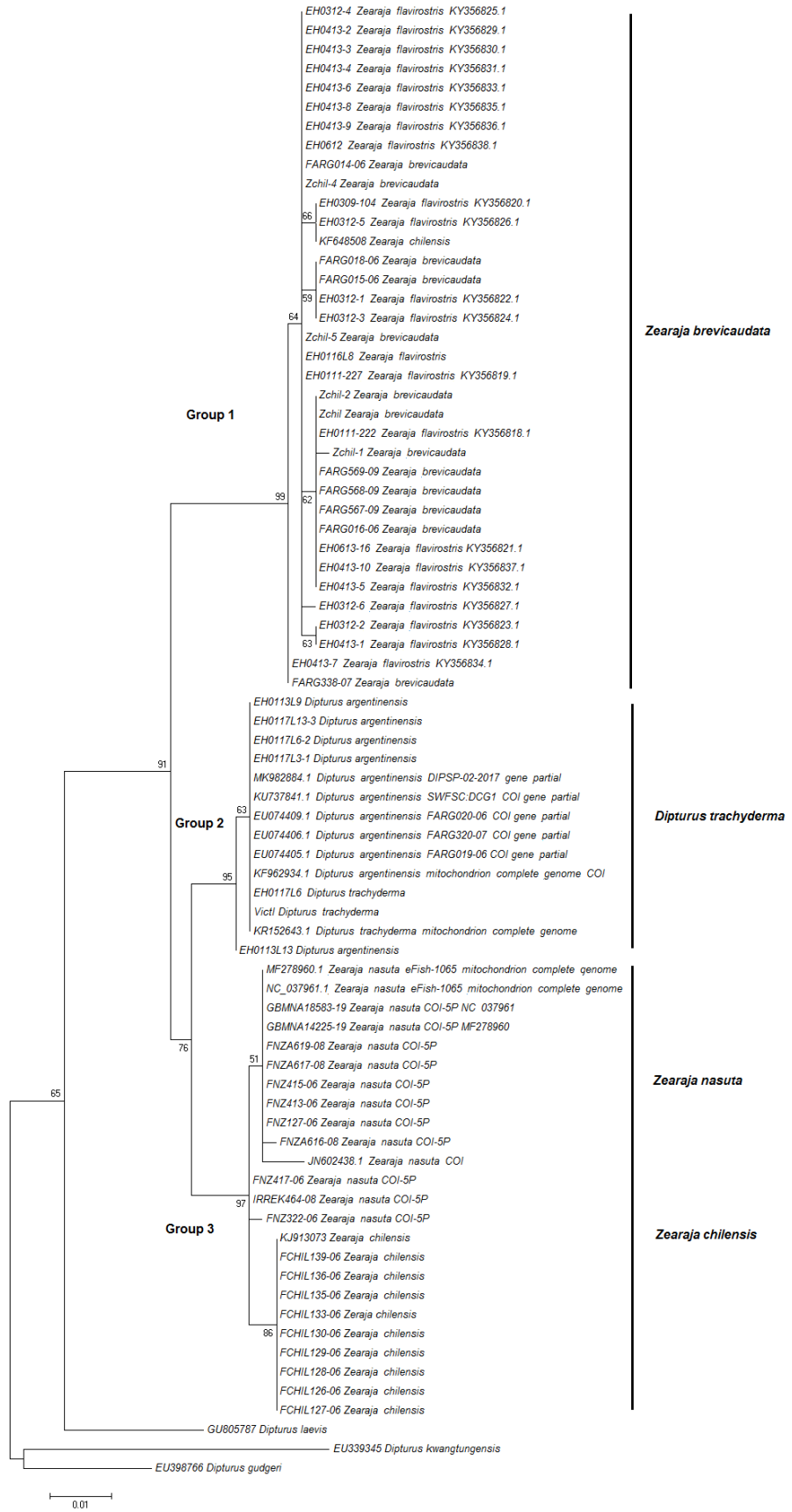

Figure 5. COI maximum likelihood tree (K2P substitution model) of *Dipturus* and *Zearaja* species. Bootstrap proportions (1000 replicates) ≥50% are displayed for all nodes.

Table 3. Interspecific K2P distances of Cytochrome Oxidase Subunit I mitochondrial gene (percentages) among *Dipturus trachyderma* (D.tra), *D. argentinensis* (D.arg), *Zearaja flavirostris* (Z.fla), *D. lamillai* (D.lam), *Z. brevicaudata* (Z.bre), *Z. chilensis* (Z.chi), and *Z. nasuta* (Z.nas). Low divergences among groups considered as the same species are indicated in bold.

	D.tra	D.arg	Z.fla	D.lam	Z.bre	Z.chi	Z.nas
D.tra							
D.arg	**0.04**						
Z.fla	3.15	3.17					
D.lam	3.22	3.24	**0.24**				
Z.bre	3.22	3.23	**0.22**	**0.33**			
Z.chi	1.65	1.67	3.42	3.49	3.51		
Z.nas	1.81	1.82	3.40	3.47	3.46	0.92	

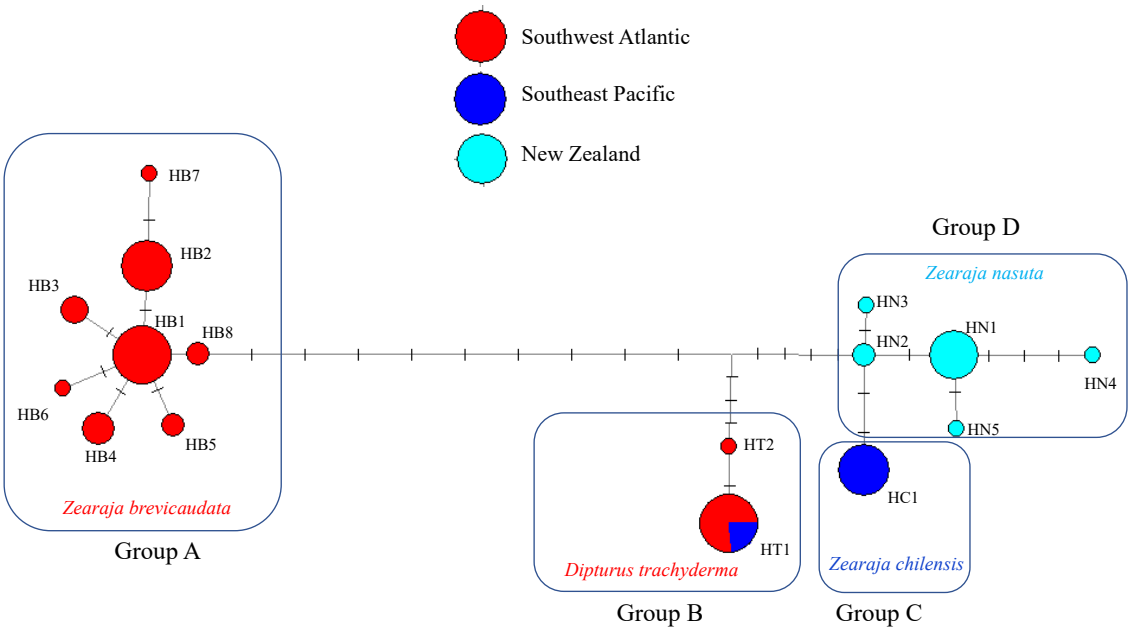

Figure 6. Median-joining network of COI haplotypes. Circle size is proportional to haplotype frequency, while connecting lines indicate mutational steps between haplotypes. HB: *Zearaja brevicaudata*, HT: *Dipturus trachyderma*, HC: *Zearaja chilensis*, HN: *Zearaja nasuta*.

3.5. Molecular Analysis of NADH2 Sequences

The analysis of the species relationship based on the NADH2 gene included a total of 26 sequences from this study and 43 sequences available online, including those used as the outgroup (Table S2).

The maximum likelihood tree topology mirrored that of the COI gene tree, revealing three well-supported clades with over 90% bootstrap values (Figure 7). Group 1 (100% bootstrap value) comprised all Atlantic sequences, corresponding to specimens classified as *D. lamillai*, *Z. brevicaudata*, and *Z. flavirostris* (Figure 7). Group 2 (95% bootstrap value) included sequences corresponding to the *D. argentinensis*, *D. trachyderma*, and *D. leptocaudus* (JQ518866.1) sequence (Figure 7). In Group 3 (78% bootstrap value), two clades differentiated *Z. nasuta* from New Zealand and *Z. chilensis* from the Pacific (Figure 7).

The interspecific K2P distance among *D. lamillai*, *D. lamillai* (KF648508.1), and *Z. flavirostris* ranged from 0.34% to 0.39% (Table 4), while the interspecific distance between *D. trachyderma*, *D. argentinensis*, and *D. leptocaudus* (JQ518866.1) ranged from 0% to 0.3% (Table 4).

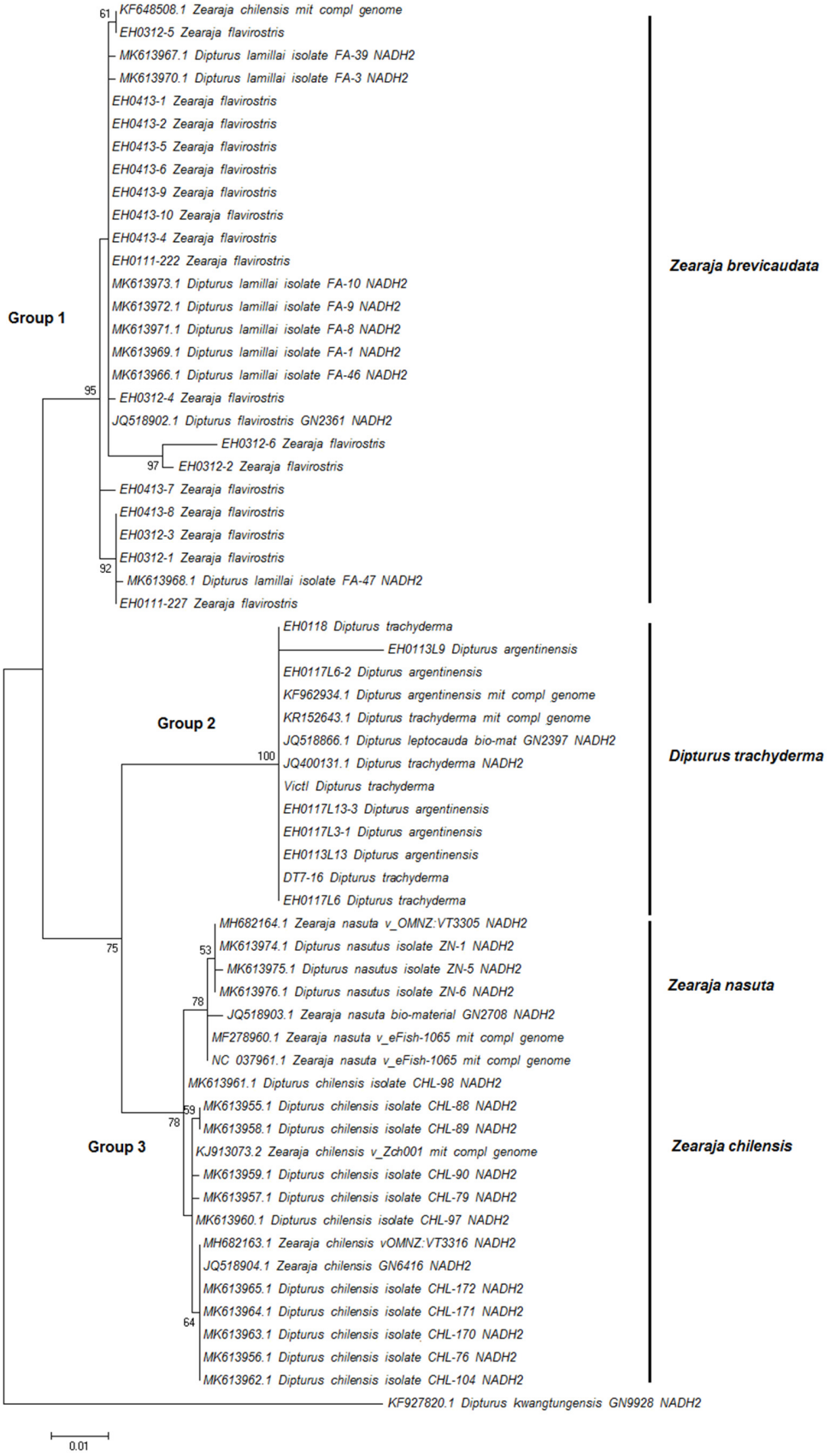

Figure 7. NADH2 maximum likelihood tree (HKY substitution model) of *Dipturus* and *Zearaja* species. Bootstrap proportions (1000 replicates) ≥50% are displayed for all nodes.

The haplotype network showed four well-differentiated haplogroups (Group A, B, C, and D, Figure 8). Group A (*Z. brevicaudata*) comprised seven haplotypes, including sequences from specimens morphologically identified as *Z. brevicaudata*, *Z. flavirostris*, and *D. lamillai* (Figure 8). This group featured sequences from the Southwest Atlantic, Falkland Islands (Malvinas), and the NADH2 from the KF648508.1 sequence of unknown origin (raw fillet collected from a restaurant in Seoul, Korea) (Figure 8). The sequences attributed to *D. lamillai* shared the haplotype HB1 with specimens previously classified as *Z. flavirostris* from Patagonia to the north of Argentina (Figure 8). Group B included two haplotypes with specimens identified as *D. trachyderma* and *D. argentinensis* (Figure 8). The haplotype HT2 comprised specimens from both the Atlantic and Pacific, including the sequence of *D. leptocaudus* from the Falkland Islands (Malvinas) (JQ518866.1) and one sequence of *D. argentinensis* with unknown provenance (KF962934.1) (Figure 8). The haplogroup C exclusively represented specimens identified as *Z. chilensis*, mostly from the Pacific, with one specimen reported in the Falkland Islands (Malvinas) (Figure 8). The haplogroup D comprised *Z. nasuta* from New Zealand (Figure 8).

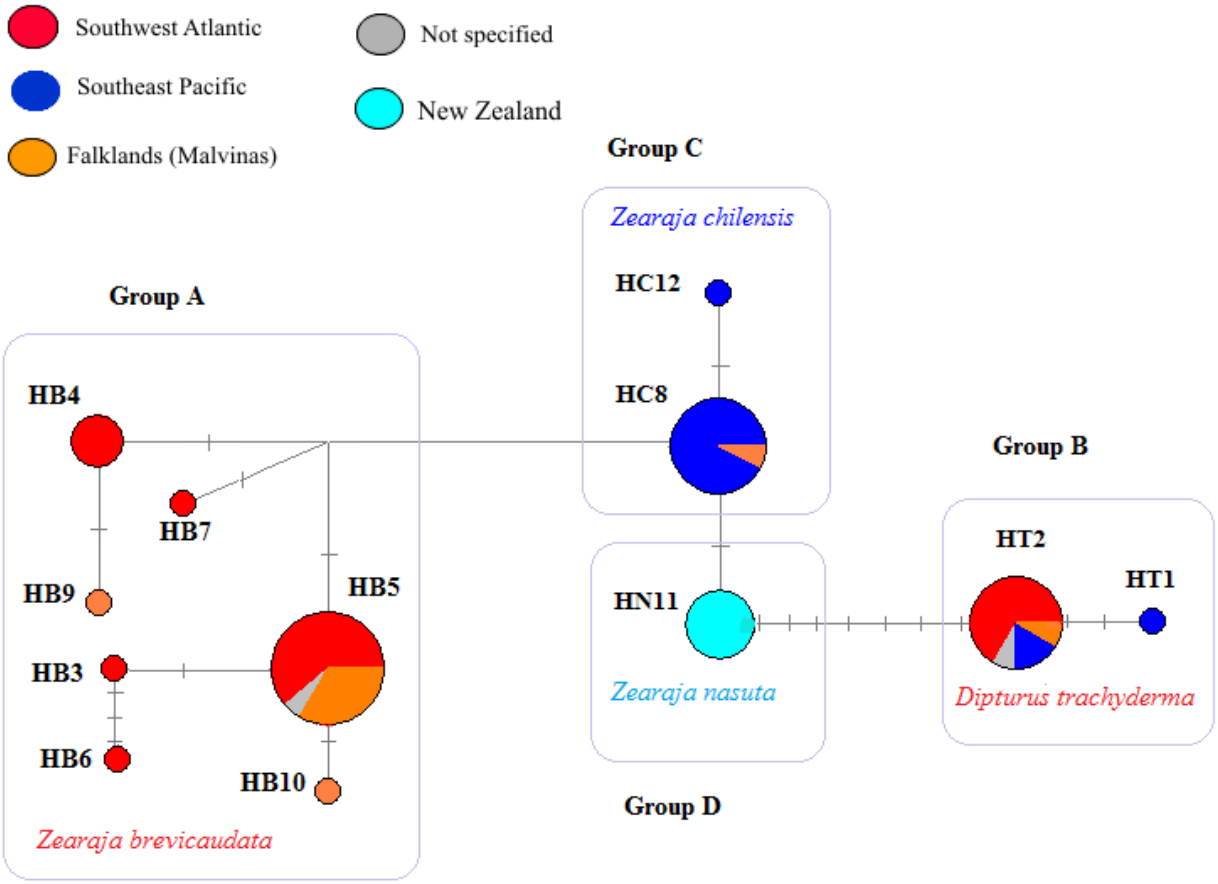

Figure 8. Median-joining network of NADH2 haplotypes. Circle size is proportional to haplotype frequency, and connecting lines indicate mutational steps between haplotypes. HB: *Zearaja brevicaudata*, HT: *Dipturus trachyderma*, HC: *Zearaja chilensis*, HN: *Zearaja nasuta*.

Table 4. Interspecific K2P distances of NADH dehydrogenase subunit 2 sequences (percentages) among *Dipturus trachyderma* (D.tra), *D. argentinensis* (D.arg), *Zearaja flavirostris* (Z.fla), *D. lamillai* (D.lam), *Z. chilensis* (Z.chi), *Z. nasuta* (Z.nas), *D. lamillai* (KF648508.1, D.lamKF) [26], and *D. leptocaudus* (JQ518866.1, D.lepJQ) [6]. Low divergences among groups considered as the same species are indicated in bold.

	D.arg	D.lepJQ	D.tra	Z.chi	Z.nas	D.lam	D.lamKF	Z.fla
D.arg								
D.lepKJQ	**0.3**							
D.tra	**0.3**	**0**						
Z.chi	4.12	3.77	3.65					
Z.nas	4.12	3.81	3.66	0.76				
D.lam	4.93	4.61	4.64	3.22	3.59			
D.lamKF	5.06	4.73	4.74	3.23	3.66	**0.23**		
Z.fla	4.96	4.62	4.66	3.32	3.64	**0.34**	**0.39**	

4. Discussion

This paper presents a comprehensive analysis of claspers, morphometrics, and both COI and NADH2 sequence data, revealing the presence of only two longnose skate species, *D. trachyderma* and *Z. brevicaudata*, south of 35 °S in the southwestern Atlantic, contrary to the previously reported six species. *Dipturus argentinensis* is a junior synonym of *D. trachyderma*, *Z. flavirostris* is a junior synonym of *Z. brevicaudata*, and the synonymization of *D. lamillai* with *Z. brevicaudata* by Gabbanelli et al. [3] is confirmed. *Dipturus leptocaudus* remains a northern valid species, but the specimen from the Falklands Islands (Malvinas), originally identified as *D. leptocaudus*, is a misidentification of *D. trachyderma*. *Zearaja brevicaudata* emerges as the most frequent and abundant species of Rajidae south of 35 °S [34,35]. The presence of *D. leptocaudus* around the Falkland Islands (Malvinas) likely resulted from misidentification, as the original description was based on juveniles from southern Brazil [8]. These juveniles were similar in size and spinulation pattern compared to the specimens analyzed by Díaz de Astarloa et al. [11] as *D. argentinensis*, exhibiting only one dorsal row of thorns on the tail [2]. In contrast, the juveniles of *D. trachyderma* displayed a single dorsal line of tail thorns, with the number of rows increasing as ontogeny progressed, in accordance with Leible and Stehmann [9].

In the phylogenetic analyses of NADH2 and COI, the sequences of *Z. flavirostris* [33], *Z. brevicaudata* [7], and a yellownose skate based on a raw fillet sample from a restaurant collected in Seoul, Korea [26], consistently clustered with the specimen of *D. lamillai* [5] from the Southwest Atlantic in the resulting NJ trees. This clustering supports their conspecificity, and according to the resurrection performed by Gabbanelli et al. [7], they should be classified as *Z. brevicaudata*, following the description of Marini [36], who was the first to describe the species in the southwestern Atlantic in 1928 [37]. This is consistent with previous molecular analyses suggesting that the Atlantic specimens might constitute a distinct species not identical to *Z. chilensis* from the Pacific [4,6,33,38,39]. These findings are also in line with the results of Concha et al. [5], who identified *D. lamillai* in the southwestern Atlantic as a new cryptic species distinct from the Pacific specimens, and with Gabbanelli et al. [3], who synonymized *D. lamillai* and *Z. brevicaudata*.

Similarly, the ML trees and haplotype networks resulting from the analysis of NADH2 and COI data showed that the juveniles *D. argentinensis*, *D. trachyderma*, and the specimen of *D. leptocaudus* (JQ518866.1) published by Naylor et al. [6] grouped together. This suggests that these specimens correspond to different ontogenetic stages of the same species. All specimens of *D. argentinensis* described to date, including the holotypes [11], were juveniles. This observation suggests that *D. argentinensis* is a junior synonym of the giant roughskin skate *D. trachyderma*. This finding aligns with previous molecular analyses that identified the sequence of *D. trachyderma* as *D. argentinensis* [13,14,40]. In this sense, the specimen of *D. leptocaudus* cited for the Falkland Islands (Malvinas) by Naylor et al. [6] is likely due to a misidentification of a juvenile of *D. trachyderma*. This confirms the northern

distribution of *D. leptocaudus* and its absence in the waters around the Falkland Islands (Malvinas). Furthermore, *D. argentinensis* and *D. trachyderma* exhibited a closer relationship to *Z. chilensis* and *Z. nasuta* from the Pacific than to *Z. brevicaudata*. This result is partially in agreement with Weigmann [12], who suggested that *D. argentinensis* should be classified under *Zearaja* due to its genetic proximity (1.5%) to *Z. chilensis*. Similarly, Vargas-Caro et al. [10] proposed that this particular clade may represent a sister-cryptic species complex or suggest the potential hybridization between *D. trachyderma* and *Z. chilensis*. According to Naylor et al. [41], the *Z. nasuta* group from New Zealand is a sister taxon to *Z. chilensis* from Chile.

Based on clasper morphology [4,7] and molecular and morphometric work in progress (P. Last and G. Naylor, pers. comm. in [42]), some *Dipturus* species have been reassigned to the genus *Zearaja*. Other authors have suggested that the genus *Zearaja* should be considered a junior synonym of *Dipturus* [5], or that they should not be considered separate genera [12,13]. However, a comprehensive review of rajid skates [2] has indicated that the genus *Dipturus* is polyphyletic, comprising several presently unrecognized genera. While our study has also shown *Zearaja* as polyphyletic, more comprehensive analyses, encompassing all *Zearaja* and *Dipturus* species worldwide, are needed to definitively confirm this hypothesis. The main morphological characteristic distinguishing *Dipturus* and *Zearaja* species is clasper morphology [4]. In the present study, we provided the clasper characteristics of the giant Atlantic roughskin skate *D. trachyderma*, which clearly align with *Dipturus*, exhibiting cartilage at1 with the distal portion called sentinel (absent in *Zearaja*). Furthermore, the claspers of *D. trachyderma* have longer vt (distal end called funnel) and dt2 cartilages than *Zearaja*, with the distal lobe not spatulate, consistent with the characteristics of *Dipturus*. In this context, we confirm the placement of the giant Atlantic roughskin skate *D. trachyderma* in the genus *Dipturus*, based on the clasper diagnosis, its similarity with the Pacific *D. trachyderma* clasper, and the observed differences with the *Zearaja* species proposed by Last and Gledhill [4].

In conclusion, our morphological and genetic analyses support the identification of *Z. brevicaudata* and *D. trachyderma* as the species inhabiting the continental shelf off the southwestern Atlantic shelf south of 35 °S. We observed only one specimen of *Z. chilensis* in the Falkland Islands (Malvinas), indicating an uncommon occurrence of this eastern Pacific skate within the southern Southwest Atlantic. We have demonstrated that *D. argentinensis* is a junior synonym of *D. trachyderma*, and *Z. flavirostris* is a junior synonym of *Z. brevicaudata*. *Dipturus leptocaudus* (Krefft and Stehmann, 1975) remains a northern valid species, but the specimen from the Falkland Islands (Malvinas) was recognized as a misidentification of *D. trachyderma*. The synonymization of *D. lamillai* with *Z. brevicaudata* by Gabbanelli et al. [3] is also confirmed. Furthermore, the clasper morphology of the Atlantic *D. trachyderma* corresponds to those from the Pacific, exhibiting the characteristic at1 cartilage of the genus *Dipturus*. This clarification provides valuable insights for the conservation and sustainable exploitation of these species, which hold significant commercial interest. We acknowledge the ongoing need for more global detailed investigations of the large, brown, long-nosed skates. For example, the enigmatic case of *Dipturus intermedius* (Parnell, 1837), which exhibits a more confined, coastal distribution than previously assumed, despite the extensive history of research in the northeastern Atlantic, highlights the intricacies and challenges inherent to the taxonomy of these species [43]. Further comprehensive studies are imperative to enhance our understanding of the diversity and distribution of *Dipturus* and *Dipturus*-like taxa worldwide. Particularly, in the Southwest Atlantic, which comprises two biogeographic provinces where the diversity of skates is notable [44]. In this region, a wide range of skates can be found, from the largest in the world (*Dipturus trachyderma*) to one of the smallest (*Psammobatis rutrum*) [44]. It includes two endemic genera (*Atlantoraja* and *Rioraja*) and several cosmopolitan genera, with one of them showing a surprising radiation (*Bathyraja*) and another (*Zearaja*) considered Gondwanan [12,44]. Moreover, a deeper understanding of skate biodiversity, along with accurate species definitions, are crucial for the development of effective fisheries management measures.

Supplementary Materials: The following Supporting Information can be downloaded at: https://www.mdpi.com/article/10.3390/d16030146/s1, Table S1: COI sequences of analyzed specimens used for phylogenetic analyses, indicating the original classification, geographic sample provenance, and references; Table S2: NADH2 sequences of analyzed specimens used for phylogenetic analyses, indicating the original classification, geographic sample provenance, and references; Table S3: Variable sites resulting from the multiple alignment among COI sequences, showing the different haplotypes obtained in this study. Grey shading indicates haplotypes grouping; Table S4: Variable sites resulting from the multiple alignment among NADH2 sequences, showing the different haplotypes obtained in this study. References [45–50] are cited in the Supplementary Materials.

Author Contributions: Conceptualization, D.E.F., M.B., G.A., S.I., N.B., M.P.-L., A.M.D.W., J.H.C. and M.I.T.; Data curation, D.E.F., M.B., G.A., S.I., N.B., A.M.D.W. and M.I.T.; Formal analysis, D.E.F., M.B., G.A., S.I., N.B., M.P.-L. and M.I.T.; Investigation, D.E.F., M.B., G.A., S.I., N.B., J.H.C. and M.I.T.; Methodology, D.E.F., M.B., G.A., S.I., A.M.D.W., J.H.C. and M.I.T.; Project administration, D.E.F., M.B., J.H.C. and M.I.T.; Resources, D.E.F., M.B., J.H.C. and M.I.T.; Software, M.B., S.I., M.P.-L. and M.I.T.; Supervision, D.E.F., M.B., G.A., M.P.-L., A.M.D.W., J.H.C. and M.I.T.; Validation, D.E.F., M.B., S.I., N.B., M.P.-L., A.M.D.W., J.H.C. and M.I.T.; Visualization, D.E.F., M.B., S.I., A.M.D.W., J.H.C. and M.I.T.; Writing—original draft, D.E.F., M.B., S.I., J.H.C. and M.I.T.; Writing—review and editing, D.E.F., M.B., G.A., S.I., N.B., M.P.-L., A.M.D.W., J.H.C. and M.I.T. All authors have read and agreed to the published version of the manuscript.

Funding: This research received no external funding.

Institutional Review Board Statement: Not applicable.

Data Availability Statement: The datasets generated and/or analyzed during the current study are available from the corresponding author on reasonable request.

Acknowledgments: We extend our heartfelt gratitude to Marcela Tobio and Cecilia Ravalli (Gabinete de Fotografía, INIDEP) for their invaluable contribution of the photographs that enrich this paper. We are also deeply grateful to Matías Landi and their team of the Instituto Radiológico, Mar del Plata, for their assistance in taking the radiographs. Our sincere appreciation goes to Montserrat Pérez Rodríguez from the Instituto Español de Oceanografía for her meticulous review of the manuscript and valuable suggestions.

Conflicts of Interest: The authors declare no conflicts of interest.

References

1. Ebert, D.; Compagno, L. Biodiversity and systematics of skates (Chondrichthyes: Rajiformes: Rajoidei). *Environ. Biol. Fishes* **2007**, *80*, 111–124. [CrossRef]
2. Last, P.R.; White, W.T.; de Carvalho, M.R.; Séret, B.; Stehmann, M.F.W.; Naylor, G.J.P. *Rays of the World*, 1st ed.; CSIRO Publishing: Melbourne, Australia, 2016; pp. 1–790.
3. Gabbanelli, V.; Naylor, G.; Weigmann, S.; Yang, L.; Vazquez, D.M.; Last, P.; Díaz de Astarloa, J.M.; Mabragaña, E. Morphological and molecular evidence reveals *Zearaja brevicaudata* (Marini, 1933) is a senior synonym of *Dipturus lamillai* Concha, Caira, Ebert & Pompert. *Zool. Stud.* **2022**, *61*, 76.
4. Last, P.R.; Gledhill, D.C. The Maugean Skate, *Zearaja maugeana* sp. nov. (Rajiformes: Rajidae)—A micro-endemic, Gondwanan relict from Tasmanian estuaries. *Zootaxa* **2007**, *1494*, 45–65. [CrossRef]
5. Concha, F.J.; Caira, J.; Ebert, D.A.; Pompert, J.H.W. Redescription and taxonomic status of *Dipturus chilensis* (Guichenot, 1848), and description of *Dipturus lamillai* sp. nov. (Rajiformes: Rajidae), a new species of long-snout skate from the Falkland Islands. *Zootaxa* **2019**, *4590*, 501–524. [CrossRef] [PubMed]
6. Naylor, G.J.P.; Caira, J.N.; Jensen, K.; Rosana, K.A.M.; White, W.T.; Last, P.R. A DNA sequence-based approach to the identification of sharks and ray species and its implications for global elasmobranch diversity and parasitology. *Bull. Am. Mus. Nat. Hist.* **2012**, *367*, 1–262. [CrossRef] [PubMed]
7. Gabbanelli, V.; Díaz de Astarloa, J.; González-Castro, M.; Vázquez, D.; Mabragaña, E. Almost a century of oblivion: Integrative taxonomy allows the resurrection of the longnose skate *Zearaja brevicaudata* (Marini, 1933) (Rajiformes; Rajidae). *Comptes Rendus Biol.* **2018**, *341*, 454–470. [CrossRef] [PubMed]
8. Krefft, G.; Stehmann, M. Ergebnisse der Forschungsreisen des FFS "Walter Herwig" nach Südamerika. XXXVI. Zwei weitere neue Rochenarten aus dem Südwestatlantik *Raja (Dipturus) leptocaudus* und *Raja (Dipturus) trachyderma* spec. nov. (Chondrichthyes, Batoidei, Rajidae). *Arch. Fischereiwiss.* **1975**, *26*, 77–97.

9. Leible, M.D.; Stehmann, M. First records of *Raja (Dipturus) trachyderma* Krefft & Stehmann, 1975 from the Southeastern pacific off Chile, with first descriptions of its clasper characters and additional skeletal and morphological details (Pisces, Rajiformes, Rajidae). *Stud. Neotrop. Fauna Environ.* **1987**, *22*, 169–188.
10. Vargas-Caro, C.; Bustamante, C.; Lamilla, J.; Bennett, M.B.; Ovenden, J.R. The phylogenetic position of the roughskin skate *Dipturus trachyderma* (Krefft & Stehmann, 1975) (Rajiformes, Rajidae) inferred from the mitochondrial genome. *Mitochondr. DNA* **2016**, *27*, 2965–2966.
11. Díaz de Astarloa, J.; Mabragaña, E.; Hanner, R.; Figueroa, D.E. Morphological and molecular evidence for a new species of longnose skate (Rajiformes: Rajidae: *Dipturus*) from Argentinean waters based on DNA barcoding. *Zootaxa* **2008**, *1291*, 35–46. [CrossRef]
12. Weigmann, S. Annotated checklist of the living sharks, batoids and chimaeras (Chondrichthyes) of the world, with a focus on biogeographical diversity. *J. Fish Biol.* **2016**, *88*, 837–1037. [CrossRef] [PubMed]
13. Carugati, L.; Melis, R.; Cariani, A.; Cau, A.; Crobe, V.; Ferrari, A.; Follesa, M.C.; Geraci, M.L.; Iglésias, S.P.; Pesci, P.; et al. Combined COI barcode-based methods to avoid mislabeling of threatened species of deep-sea skates. *Anim. Conserv.* **2022**, *25*, 38–52. [CrossRef]
14. Concha, F.J. A Taxonomic Resource of South American Skates and Its Conservation Implications. Ph.D. Thesis, University of Connecticut, Storrs, CT, USA, 2021.
15. Walker, T.I. Reproduction in fisheries science. In *Reproductive Biology and Phylogeny of Chondrichthyes: Sharks, Rays and Chimaeras*; Hamlett, W.C., Ed.; Science Publishers: Enfield, CT, USA, 2005; pp. 81–127.
16. Colonello, J.H.; Christiansen, E.H.; Macchi, G.J. Escala de madurez sexual para peces cartilaginosos de la Plataforma Continental Argentina. In *Contribuciones Sobre Biología, Pesca y Comercialización de Tiburones en la Argentina. Aportes Para la Elaboración del Plan de Acción Nacional*; Wöhler, O.C., Cedrola, P., Cousseau, M.B., Eds.; Consejo Federal Pesquero: Buenos Aires, Argentina, 2011; pp. 115–128.
17. Stehmann, M.F.W. Proposal of a maturity stages scale for oviparous and viviparous cartilaginous fishes (Pisces, Chondrichthyes). *Arch. Fish. Mar. Res.* **2002**, *50*, 23–48.
18. Weigmann, S.; Reinecke, T. Additions to the Taxonomy of the Antarctic Dark-Mouth Skate *Bathyraja arctowskii* (Dollo, 1904), with Descriptions of the Syntypes and Morphology of Teeth, Dermal Denticles and Thorns. *Diversity* **2023**, *15*, 899. [CrossRef]
19. Lleonart, J.; Salat, J.; Torres, G.J. Removing allometrics effects of body size in morphological analysis. *J. Theor. Biol.* **2000**, *205*, 85–93. [CrossRef] [PubMed]
20. Krebs, C.J. *Ecological Methodology*, 1st ed.; Harper Collins: Nueva York, NY, USA, 1989; pp. 1–654.
21. Zuur, A.F.; Ieno, E.N.; Smith, G.M. *Analysing Ecological Data*; Springer: Berlin, Germany, 2007; pp. 1–672.
22. Figueroa, D.E. Clave ilustrada de agnatos y peces cartilaginosos de Argentina y Uruguay. In *Contribuciones Sobre Biología, Pesca y Comercialización de Tiburones en la Argentina. Aportes Para la Elaboración del Plan de Acción Nacional*; Wöhler, O.C., Cedrola, P., Cousseau, M.B., Eds.; Consejo Federal Pesquero: Buenos Aires, Argentina, 2011; pp. 25–74.
23. Andreoli, G.; Trucco, M.I. Evaluación de diferentes protocolos de extracción de ADN en muestras de músculo de espina dorsal en *Mustelus schmitti*. *Inf. Investig. INIDEP* **2012**, *7*, 1–8.
24. Ward, R.; Zemlak, T.; Innes, B.; Last, P.; Hebert, P. DNA barcoding Australia's fish species. *Philos. Trans. R. Soc. Lond. B* **2005**, *360*, 1847–1857. [CrossRef]
25. Naylor, G.J.; Ryburn, J.A.; Fedrigo, O.; Lopez, J.A. Phylogenetic relationships among the major lineages of modern elasmobranchs. In *Reproductive Biology and Phylogeny 3*; Hamlett, W.C., Jamieson, B.G.M., Eds.; Science Publishers: Enfield, CT, USA, 2005; pp. 1–25.
26. Jeong, D.; Lee, Y.H. Complete mitochondrial genome of the yellownose skate: *Zearaja chilensis* (Rajiformes. Rajidae). *Mitochondr. DNA* **2014**, *27*, 293–294. [CrossRef]
27. Hall, T.A. BioEdit: A user-friendly biological sequence alignment editor and analysis program for Windows 95/98/NT. *Nucl. Acids Symp. Ser.* **1999**, *41*, 95–98.
28. Larkin, M.A.; Blackshields, G.; Brown, N.P.; Chenna, R.; McGettigan, P.A.; McWilliam, H.; Higgins, D.G. Clustal W and Clustal X version 2.0. *Bioinformatics* **2007**, *23*, 2947–2948. [CrossRef]
29. Kimura, M. A simple method of estimating evolutionary rate of base substitutions through comparative studies of nucleotide sequences. *J. Mol. Evol.* **1980**, *16*, 111–120. [CrossRef]
30. Tamura, K.; Stecher, G.; Peterson, D.; Filipski, A.; Kumar, S. MEGA6: Molecular Evolutionary Genetics Analysis version 6.0. *Mol. Biol. Evol.* **2013**, *30*, 2725–2729. [CrossRef]
31. Librado, P.; Rozas, J. DnaSP v5. A software for comprehensive analysis of DNA polymorphism data. *Bioinformatics* **2009**, *25*, 1451–1452. [CrossRef] [PubMed]
32. Bandelt, H.J.; Forster, P.; Röhl, A. Median-joining networks for inferring intraspecific phylogenies. *Mol. Biol. Evol.* **1999**, *16*, 37–48. [CrossRef] [PubMed]
33. Izzo, S.; Andreoli, G.; Figueroa, D.E.; Costagliola, M. Molecular characterization of sympatric skates of the *Dipturus* and *Zearaja* genera of the Argentine Sea with DNA Barcode. *Rev. Investig. Desarr. Pesq.* **2017**, *31*, 55–74.
34. Colonello, J.H.; Cortés, F. Parámetros reproductivos de la raya *Dipturus chilensis* en el Atlántico Sudoccidental (34°–48° S). *Ser. INIDEP Inf. Téc.* **2014**, *92*, 1–19.

35. Cortés, F.; Colonello, J.H.; Sammarone, M.; Zavatteri, A.; Hozbor, N.M. Demographic analyses reveal differential biological vulnerability in four Southwestern Atlantic skates. *Can. J. Fish. Aquat. Sci.* **2023**, *80*, 851–865. [CrossRef]
36. Marini, T.L. Rectificando errores ictiológicos. *Physis* **1933**, *11*, 328–332.
37. Marini, T.L. Nota sobre dos rayas nuevas para la costa atlántica de la provincia de Buenos Aires. *Physis* **1928**, *9*, 133–141.
38. Gomes, U.L.; Picado, S.S. Distribution of the species of *Dipturus* Rafinesque (Rajidae, Rajinae, Rajini) off Brazil and first record of the Caribbean skate *D. teevani* (Bigelow & Schroeder), in the Western South Atlantic. *Rev. Bras. Zool.* **2001**, *18*, 171–185.
39. Vargas-Caro, C.; Bustamante, C.; Bennett, M.B.; Ovenden, J.R. The complete validated mitochondrial genome of the yellownose skate *Zearaja chilensis* (Guichenoti 1848) (Rajiformes. Rajidae). *Mitochondr. DNA* **2014**, *27*, 1227–1228. [CrossRef] [PubMed]
40. Izzo, S.; Andreoli, G.; Trucco, M.I. Obtención de marcadores moleculares por RFLP (Polimorfismos en el Largo de Restricción) para la identificación de rayas comerciales. *INIDEP. Inf. Investig.* **2019**, *47*, 1–11.
41. Naylor, G.J.P.; Caira, J.N.; Jensen, K.; Rosana, K.A.M.; Straube, N.; Lakner, C. Elasmobranch Phylogeny: A Mitochondrial Estimate Based on 595 Species. In *The Biology of Sharks and Their Relatives*; Carrier, J.C., Musick, J.A., Heithaus, M.R., Eds.; CRC Press: Boca Raton, FL, USA, 2012; pp. 31–56.
42. Awruch, C.A.; Bell, J.D.; Semmens, J.M.; Lyle, J.M. Life history traits and conservation actions for the Maugean skate (*Zearaja maugeana*), an endangered species occupying an anthropogenically impacted estuary. *Aquatic. Conserv. Mar. Freshw. Ecosyst.* **2021**, *31*, 2178–2192. [CrossRef]
43. Garbett, A.; Loca, S.L.; Barreau, T.; Biscoito, M.; Bradley, C.; Breen, J.; Clarke, M.; Ellis, J.R.; Griffiths, A.M.; Hannon, G.; et al. A holistic and comprehensive data approach validates the distribution of the critically endangered flapper skate (*Dipturus intermedius*). *J. Fish Biol.* **2023**, *103*, 516–528. [CrossRef]
44. Figueroa, D.E.; Barbini, S.A.; Belleggia, M.; Sabadin, D.E.; Román, J.M.; De Wysiecki, A.M. The ichthyofaunistic colonization and complex biogeographic history of the southern portion of the Southwest Atlantic Ocean. *Mar. Ecol.* **2023**, *44*, e12742. [CrossRef]
45. Mabragaña, E.; Diaz de Astarloa, J.; Hanner, R.; Zhang, J.; Gonzalez Castro, M. DNA barcoding identifies argentine fishes from marine and brackish waters. *PLoS ONE* **2011**, *6*, e28655. [CrossRef] [PubMed]
46. Vargas Caro, C.A. Skate-Ing on Thin Ice: Molecular Ecology of Longnose Skates in the Southeast Pacific Ocean. Ph.D. Thesis, University of Queensland, Brisbane, Australia, 2017.
47. Lago, F.C.; Vieites, J.M.; Espiñeira, M. Development of a FINS- based method for the identification of skates species of commercial interest. *Food Control* **2012**, *24*, 38–43. [CrossRef]
48. Ward, R.; Holmes, B.; Last, P. DNA barcoding Australasian chondrichthyans: Results and potential uses in conservation. *Mar. Freshw. Res.* **2008**, *59*, 57–71. [CrossRef]
49. Beer, A.; Ingram, T.; Randhawa, H.S. Role of ecology and phylogeny in determining tapeworm assemblages in skates (Rajiformes). *J. Helminthol.* **2019**, *93*, 738–751. [CrossRef]
50. Straube, N.; White, W.T.; Ho, H.-C.; Rochel, E.; Corrigan, S.; Li, C.; Naylor, G.J.P. A DNA sequence-bases identification checklist for Taiwanese chondricthyans. *Zootaxa* **2013**, *3752*, 256–278. [CrossRef]